Environmental Science Nano

ROYAL SOCIETY OF CHEMISTRY

PAPER

View Article Online
View Journal | View Issue

Cite this: *Environ. Sci.: Nano*, 2026, **13**, 1730

The effect of polystyrene nanoplastic on ion channels and mucus secretion – insights from Caco-2 cell model

Gabriela Weglinska, Jakub Hoser, Piotr Bednarczyk and Miroslaw Zajac *

Received 15th December 2025,
Accepted 19th February 2026

DOI: 10.1039/d5en01169h

rsc.li/es-nano

Plastic pollution is an escalating global concern, as the degradation of plastic waste generates micro- and nanoplastics that can be ingested by living organisms and interact with the intestinal epithelial barrier. However, the effects of nanoplastics on human intestinal epithelial function, particularly with respect to transepithelial ion transport, remain insufficiently understood. To better understand the effects of nanoplastics on the intestinal epithelium, we aimed to investigate the impact of 100 nm polystyrene nanoplastics (PS-NPs) on mucus secretion, ion transport, and epithelial integrity in the human intestinal epithelial cell line Caco-2. The cellular response to nanoplastic exposure was assessed by measuring cytotoxicity, transepithelial electrical resistance (TEER), and cell migration. Transepithelial ion transport was assessed in Ussing chamber system on treated and untreated Caco-2 cell monolayers, and the activity of specific ion-channels was analysed using selective pharmacological modulators. Despite some alterations, nanoplastic exposure did not exert marked cytotoxic effects, changes in barrier integrity, and in cell migration. Ion transport analysis revealed decreased CFTR activity and enhanced CaCC activity in nanoplastic-treated cell monolayers. Nanoplastic exposure also induced an increase in mucus secretion. These findings suggest that polystyrene nanoplastics modulate intestinal epithelial ion transport and stimulate mucus secretion, which may be associated with TMEM16A activation. This response may represent a protective mechanism of intestinal epithelial cells against nanoplastic exposure.

Environmental significance

As plastic debris fragments into micro- and nanoplastics, human exposure through food and water is increasingly unavoidable, raising concerns about intestinal health. This study demonstrates that environmentally relevant concentrations of 100 nm polystyrene nanoplastics alter key physiological functions of the human intestinal epithelium. Exposure increased mucus secretion and disrupted transepithelial ion transport, characterized by reduced CFTR activity and enhanced TMEM16A activity. Because mucus secretion is essential for maintaining the intestinal protective barrier, these findings indicate that nanoplastics can directly influence epithelial defense mechanisms. By identifying ion channel modulation as a response to nanoplastic exposure, this work provides new insight into how plastic pollution may affect gut homeostasis and highlights the importance of incorporating epithelial function into environmental and human health risk assessments.

1. Introduction

In 2021, global plastic production reached approximately 390.7 million tonnes,[1] with projections suggesting a potential fourfold increase by 2050.[2] The massive scale of plastic production, combined with its resistance to degradation and insufficient recycling, has led to its widespread environmental distribution.[3] The accumulation of plastic waste has increased levels of micro- (MPs) and nanoplastics (NPs), collectively termed micro- and nanoplastics (MNPs).[4] Through degradation processes, plastics fragment into smaller particles with greater persistence, mobility, and biological reactivity.[5] As a result, MNPs are now widespread in air, water, and soil, increasing human exposure *via* ingestion, inhalation, and dermal penetration.[6] Among these, oral ingestion is considered the primary route of MNPs' entry into the human body.[7] It is estimated that an average person ingests between 39 000 and 52 000 plastic particles annually.[8] Once ingested, nanoparticles can reach the intestinal lumen, where they interact with gastrointestinal fluids, the mucus layer, microbiota, and the epithelial barrier, potentially enabling their translocation.[9]

The intestinal epithelium serves as a crucial barrier against toxins and pathogens, consisting of the mucosal epithelium, mucus, microbiota, immunoglobulins, and digestive fluids.[10,11]

Department of Physics and Biophysics, Institute of Biology, Warsaw University of Life Sciences, 02-776 Warsaw, Poland. E-mail: miroslaw_zajac@sggw.edu.pl

Epithelial cells form a barrier *via* tight junctions (TJs) and regulate paracellular and transcellular transport of small molecules. The intestinal mucus layer, produced mainly by goblet cells and enterocytes, is essential for gut protection and homeostasis,[12] and its properties are tightly regulated by ion-transporting proteins. Ion channels therefore play a crucial role in rapidly adapting mucus to maintain its protective and functional roles.[10,12] Among them, the cystic fibrosis transmembrane conductance regulator (CFTR) and calcium-activated chloride channels (CaCCs) are particularly important.[13] CFTR, the principal chloride-secreting channel at the apical epithelial surface, also regulates the activity of other ion transporting proteins. In addition to chloride, CFTR secretes bicarbonate ions, maintaining extracellular pH and enabling mucin expansion.[14] TMEM16A, a member of the CaCC family, regulates intracellular Ca^{2+} localization, promotes CFTR activation through adenylyl cyclase, protein kinase A (PKA), and tyrosine kinase signaling, and facilitates mucin exocytosis — making it essential for mucus secretion.[15]

Although research on nanoplastics and gut health is expanding, most work has focused on inflammation, oxidative stress, barrier disruption (TJs), and microbiota alterations. By contrast, studies specifically investigating their impact on intestinal ion transport remain scarce. To date, electrophysiological approaches have not been applied, providing a novel perspective. This study addresses the critical gap in understanding the effects and potential hazards of polystyrene nanolastics (PS-NPs) on the intestinal epithelium. Using Caco-2 cells as a physiological model of the intestinal barrier, we investigated cellular responses to exposure to 100 nm PS-NPs. PS-NPs were selected, as polystyrene accounts for approximately 7–10% of global plastic production and is extensively used in food packaging, consumer products, aquaculture, electronics, and automotive applications.[16] The size of 100 nm was selected as it is small enough to interact with cellular membranes, undergo endocytosis, and potentially cross biological barriers, yet remain experimentally detectable and well-characterized. Their commercial availability and stable, reproducible physicochemical properties make them suitable for standardized *in vitro* toxicity and mechanistic studies.[17] We examined the potential of PS-NPs to modulate ion channel activity, with a particular focus on CFTR and TMEM16A, and assessed their effects on mucus production. These findings offer new insights into the biological mechanisms underlying nanoplastic effects *in vitro*.

2. Materials and methods

2.1. Polystyrene particles

In this study, a standardized sample of polystyrene nanoparticles obtained from Sigma-Aldrich, St. Louis, MO, USA (cat. no. 43302) and previously used by our group[18] was employed. Briefly, the sample consisted of an aqueous suspension (10% w/w) of particles with an average diameter of 100 nm and a density of 1.05 g cm^{-3}. Nanoplastic samples were maintained under sterile conditions at 2–8 °C throughout the experiments.

2.2. Cell culture

The human colon adenocarcinoma cell line Caco-2 (Sigma-Aldrich, St. Louis, MO, USA), widely used as a model of the intestinal epithelium as it spontaneously forms an integral monolayer, develop tight junctions, express brush-border enzymes, and establish active transport systems,[19,20] was employed in the experiments. During culture, they polarize and acquire morphological and functional characteristics of small intestinal enterocytes.[20] To better mimic *in vivo* conditions, in some experiments, Caco-2 cells were grown on porous supports, which enhance their differentiation.[20]

Cells were cultured in Dulbecco's modified Eagle medium (DMEM; Sigma-Aldrich, St. Louis, MO, USA) containing L-glutamine and sodium pyruvate, and supplemented with non-essential amino acids (NEAA; 10 mg mL^{-1}; Sigma-Aldrich, St. Louis, MO, USA), 10% fetal bovine serum (Gibco, Thermo Fisher Scientific, Waltham, MA, USA), and penicillin–streptomycin (10 mg mL^{-1}; Sigma-Aldrich, St. Louis, MO, USA). Cultures were maintained at 37 °C in a humidified incubator with 5% CO_2. Cells were passaged twice weekly at 70–80% confluence using 0.25% trypsin–EDTA (Sigma-Aldrich, St. Louis, MO, USA), and passages below 40 were used for the experiments.

2.3. Viability assays

To assess the viability of Caco-2 cells exposed to PS-NPs, a spectrophotometric Trypan blue exclusion assay (0.02% Trypan blue solution; MERCK, Darmstadt, Germany) was performed following Hammoudeh *et al.*[21] using a plate reader (Multiskan SkyHigh, Thermo Fischer Scientific, Waltham, MA, USA). Cells were seeded into 96-well plates at a density of 5000 cells per well and incubated with PS-NPs at concentrations of 0, 10, 50, 100, 200, and 300 μg mL^{-1} for 24, 48, and 72 hours.

2.4. The migration and proliferation assay

Effects of PS-NPs on cell migration and proliferation were assessed using the scratch assay, as previously described.[22] Caco-2 cells were seeded in 24-well plates (Sarstedt, Nümbrecht, Germany) at a density of 2.5×10^5 cells per well and cultured for 48 h to reach confluence. A linear scratch was created using sterile 100 μL pipette tips, and cells were rinsed twice with PBS to remove debris before adding fresh cell culture medium supplemented with PS-NPs at varying concentrations (0, 10, 50, 100 μg mL^{-1}). Scratch areas were monitored and photographed at 0, 3, 6, 24, and 48 h using a DLTX1080PCMOSHDU2SD camera (DELTA Optical, Mińsk Mazowiecki, Poland) mounted on an inverted optical microscope (OLYMPUS IMT-2, Tokyo, Japan). Images were saved in TIFF format using DLT Cam Viewer software and analyzed with ImageJ software (version 1.54 k). Results were expressed as the percentage of scratch area remaining at each

time point, with a decrease in scratch size indicating cell migration and proliferation.

2.5. Transepithelial electrical resistance (TEER) measurements

For barrier integrity measurements, cells were grown on porous supports. Briefly, cells cultured in flasks and reaching 80–90% confluence were rinsed by PBS and detached using 2 ml of 0.25% trypsin–EDTA (Sigma-Aldrich, St. Louis, MO, USA). Subsequently, 8 mL of fresh culture medium was added, and the cell numbers were determined using a TC20 cell counter (BioRad, Hercules, CA, USA). The cells were then transferred to 15 mL falcon tubes and centrifuged at 1500 rpm for 5 minutes. The resulting cell pellet was resuspended in fresh cell culture medium. 200 µl of cell suspension was seeded onto the apical compartment of Corning Costar Transwell inserts (TC-treated PET membrane, 0.4 µm pore size, 0.33 cm^2 surface area) at a density of 2.5×10^5 cells per insert, while the basolateral compartment was filled with 600 µL of fresh cell culture medium. The cell culture medium was changed every other day and the transepithelial electrical resistance (TEER) was measured using a Millicell ERS-2 voltohmmeter (Millipore, MERCK, Darmstadt, Germany) with STX-2 chopstick electrodes (Millipore, MERCK, Darmstadt, Germany) prior to medium replacement. Cells grown on porous support were maintained at 37 °C in a humidified incubator with 5% CO_2 for 17–21 days until TEER values stabilized above 1000 Ωcm^2. The final TEER values were calculated on the basis of the following equation: $\text{TEER} = (R - R_b) \times S$, where R [Ω] is the resistance of filter insert with cells, R_b [Ω] is the resistance of the filter alone (blanc) and S is the growth area of the filter [cm^2].

To assess the effect of PS-NPs on barrier integrity, cell monolayers were apically exposed to varying concentrations of PS-NPs (0, 10, 50, and 100 µg mL^{-1}), and TEER was measured after 24, 48, and 72 hours as previously described.

2.6. Mucus staining

For mucin detection, Caco-2 cells were seeded on both Transwell inserts (as described above) and 96-well plate (at a density of 10 000 cells per well). Confluent cells cultured on 96-well plate were exposed to PS-NPs at concentrations of 0, 10, 50, and 100 µg mL^{-1} for 72 hours. After incubation, the culture medium was removed, and the cells were washed with PBS.

Subsequently, the cell monolayers were stained with 0.2 mL of Alcian Blue solution (pH 2.5) prepared in acetic acid (MERCK, Darmstadt, Germany) which was apically added to each insert and incubated for 30 minutes at room temperature. Excess dye was removed by washing three times with PBS. Cells cultured on 96-well plate were stained using Alcian Blue – Periodic Acid Schiff method according to manufacturer's instructions (Abcam, Cambridge, UK). Stained cells were examined using an inverted optical microscope (Olympus CKX53, Olympus, Tokyo, Japan), and images were captured with a DLTX1080PCMOSHDU2SD camera (DELTA Optical, Minsk Mazowiecki, Poland). The amount of mucus produced by the cells was quantified as a percentage of stained area with ImageJ software (version 1.54 k).

2.7. Ion transport measurements

Ion channel activities of polarized cell monolayers were measured in Ussing chambers as previously described.[22] Briefly, polarized Caco-2 cell monolayers were mounted in Ussing chambers (Easy Mount Chamber system EM-CSYS, Physiologic Instruments, Reno, NV, USA) connected to a VCC MC8-8S voltage/current clamp unit (Physiologic Instruments, Reno, NV, USA). Signals were digitized and recorded using acquire and analyze module (Physiologic Instruments, Reno, NV, USA).

The experimental chambers were filled with modified Krebs–Henseleit solutions on both sides. Chloride concentration gradient across the cell monolayers was applied by differential composition of basolateral (145 mM NaCl, 3.3 mM K_2HPO_4, 10 mM HEPES, 10 mM D-glucose, 1.2 mM $MgCl_2$, 1.2 mM $CaCl_2$ and pH adjusted at 7.35) and apical medium (with 145 mM NaCl replaced by 145 mM Na-gluconate and pH adjusted at 7.35).

The experiments were performed at 37 °C using heated water jackets, the experimental solutions were bubbled with carbogen gas (95 O_2–5% CO_2) and the short circuit current (Isc) was measured under voltage clamp configuration. To investigate particular ion transporting proteins activities, the following inhibitors and activators were used: the ENaC-channel inhibitor amiloride (100 µM; Spectrum Chemical, NJ, USA) to inhibit Na^+ reabsorption; cAMP agonist forskolin (10 µM; MERCK, Darmstadt, Germany) to activate transepithelial cAMP dependent CFTR current; the specific CFTR inhibitor Inh-172 (5 µM; MERCK, Darmstadt, Germany), the specific TMEM16A inhibitor Ani-9 (9 µM; MERCK, Darmstadt, Germany), and adenosine triphosphate ATP (100 µM; MERCK, Darmstadt, Germany) to investigate purinergic calcium-dependent Cl^- secretion. To assess the effect of PS-NPs on ion transport, polystyrene nanoplastic was directly added to the apical chamber. The effect of NPs on TMEM16A activity was assessed for concentrations of 10 µg mL^{-1}, 50 µg mL^{-1}, 100 µg mL^{-1} in the absence and presence of its specific inhibitor Ani-9, while the effect on CFTR activity was assessed for the PS-NPs concentration of 100 µg mL^{-1}. Isc change after CFTR inhibition ($\Delta Isc_{Inh\text{-}172}$), following its activation by Forskolin (ΔIsc_{FRSK}), served as an index of CFTR function.

2.8. Intracellular calcium level detection

To assess changes in intracellular calcium levels, cells were seeded in 96-well plates and incubated with PS-NPs nanoplastics at concentrations of 10, 50, 100 µg mL^{-1} for 1, 24, and 48 hours. After incubation, cells were washed with DPBS (MERCK, Darmstadt, Germany) to remove residual PS-NPs. Intracellular calcium was measured using the ratiometric fluorescent dye Fura-2, according to the manufacturer's instructions. Ionomycin was used as a positive control. Fluorescence intensity was measured using a Fluoroskan Ascent microplate reader (Thermo Fisher Scientific, Waltham, MA,

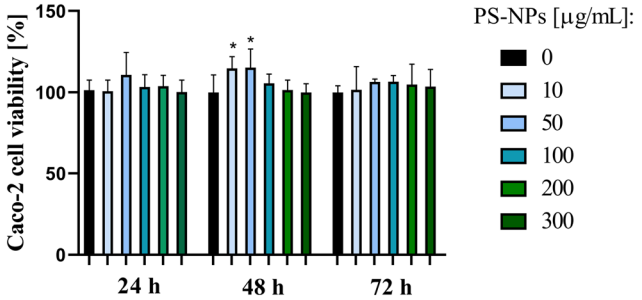

Fig. 1 Time- and dose-dependent changes in Caco-2 cell viability following PS-NP exposure. Caco-2 cell viability after exposure to PS-NPs (0, 50, 100, 200, and 300 µg mL^{-1}) for 24, 48, and 72 h, measured by the Trypan blue assay. Data are expressed as percentage values, with bars representing mean ± SD (n = 4). Statistical comparisons within each group *versus* control were performed using one-way ANOVA. Significance levels at *$p < 0.05$.

USA) at an excitation wavelength of 340 and 380 nm and an emission wavelength of 538 nm. Intracellular calcium levels were calculated as the ratio of fluorescence intensity at 340 nm to that at 380 nm (F_{340}/F_{380}), providing a quantitative measure of cytosolic calcium concentration.

2.9. Statistical analysis

Statistical analyses were performed using GraphPad Prism 8 (GraphPad Software, San Diego, CA, USA). Each experiment was repeated at least three times, and the data are presented as mean ± SD. Comparisons were performed with one-way ANOVA or Students's t-test as appropriate. Differences were considered statistically significant at *$p < 0.05$, **$p < 0.01$ or ***$p < 0.001$.

3. Results

3.1. PS-NPs slightly impact cell viability

To evaluate the potential risks of plastic cytotoxicity, the first step of this study examined Caco-2 cell viability after PS-NPs exposure at different concentrations and time points. As shown in Fig. 1, cell viability remained largely stable across treatments. Although some variations were observed compared with controls, most differences were not statistically significant. A significant increase in cell viability was detected only after 48 h exposure, where viability increased to 115 ± 7% in cells treated with 10 µg mL^{-1} and 115 ± 11% in cells treated with 50 µg mL^{-1} PS-NPs. Based on the cell viability assay results presented here, our previous study,[18] and published literature, PS-NPs concentrations of 10, 50, and 100 µg mL^{-1} were selected for subsequent experiments. Concentrations up to 100 µg mL^{-1} are commonly used in studies investigating the intestinal toxicological effects of PS-NPs, facilitating cross-study comparisons.[23,24] Additionally, plastic microparticles have been reported at levels up to 100 µg mL^{-1} in human gastrointestinal fluids.[25]

3.2. Effects of PS-NPs on cell proliferation/migration

To evaluate the effect of PS-NPs on cell proliferation and migration, a scratch assay was performed. The results, expressed as the percentage of the scratch area, are shown in Fig. 2. A slight reduction in cell proliferation was observed following PS-NPs exposure, with the most pronounced effect at the highest concentration tested (100 µg mL^{-1}). However, these differences were not statistically significant.

3.3. PS-NPs do not affect the transepithelial electrical resistance (TEER)

After confirming that PS-NPs did not induce acute cytotoxicity or affect cell proliferation, a more physiologically relevant model using Transwell inserts was established. Polarized Caco-2 cell monolayers with stable transepithelial electrical resistance (TEER) were exposed to PS-NPs at concentrations of 0, 10, 50, and 100 µg mL^{-1}, and TEER was measured after 24, 48, and 72 h. As shown in Fig. 3, none of the tested PS-NPs concentrations significantly altered TEER, although a slight increase in TEER values was observed in all PS-NPs-treated cell monolayers when compared to controls.

3.4. PS-NPs exposure results in increased mucus production

To explore the potential mechanism behind the TEER increase in PS-NP-exposed monolayers, Alcian Blue/PAS staining was

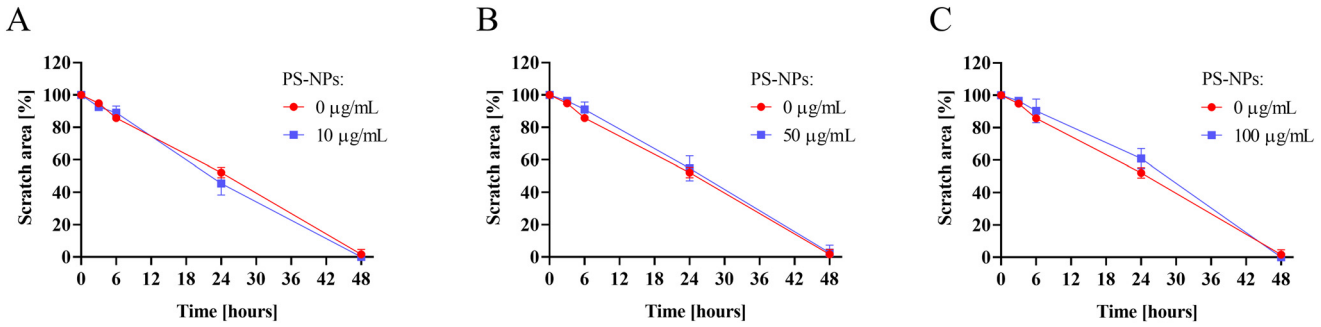

Fig. 2 PS-NP-induced changes in Caco-2 cell migration (scratch assay). Quantitative analysis of migration is expressed as the percentage of the scratch area relative to the initial time point (0 h), and was measured after 3, 6, 24, and 48 h of exposure to PS-NPs at concentrations of 10 µg mL^{-1} (A), 50 µg mL^{-1} (B), and 100 µg mL^{-1} (C). Data represents the mean scratch area ± standard deviation (SD) from three independent experiments (n = 3). Statistical significance was determined using one-way ANOVA.

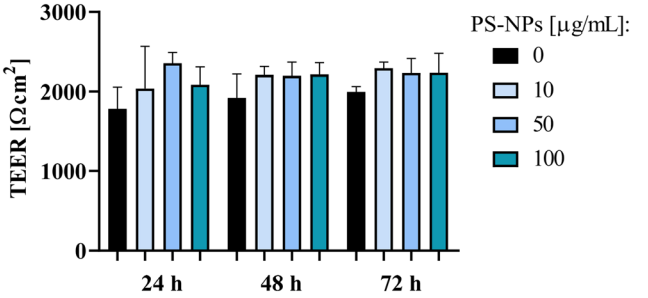

Fig. 3 Time- and dose-dependent effects of PS-NPs on TEER in Caco-2 cell monolayers. Transepithelial electrical resistance (TEER) of Caco-2 cell monolayers exposed to PS-NPs at concentrations of 0, 10, 50, and 100 µg mL^{-1} for 24, 48, and 72 h. Data are expressed as mean ± standard deviation (SD) (n = 3). Statistical significance relative to the control within each group was assessed by one-way ANOVA.

used to evaluate mucus production. Initial stainings were performed on cells cultured in 96-well plates treated with 10, 50, and 100 µg mL^{-1} PS-NPs, and a concentration-dependent increase in mucus production was observed after 72 hours of treatment (Fig. 4A and C). To better mimic the physiological environment of the intestinal epithelium, Alcian Blue staining was also performed on polarized Caco-2 monolayers exhibiting appropriate TEER values. The monolayers were treated with PS-NPs at concentrations of 10, 50, and 100 µg mL^{-1} for 72 hours prior to staining. As shown in Fig. 4B and D, mucus production increased in a PS-NP concentration-dependent manner. At the highest concentration tested (100 µg mL^{-1}), visible mucus clumps were observed, indicating that PS-NPs stimulate mucus production in Caco-2 cells.

3.5. Measurements of ion transport across Caco-2 cell monolayers exposed to PS-NPs

To investigate whether PS-NPs affect ion transport across Caco-2 monolayers, short-circuit current measurements were performed. Initial findings showed that PS-NPs exerted a modest inhibitory effect on CFTR channel activity. As shown in Fig. 5A, acute addition of 100 µg mL^{-1} PS-NPs reduced CFTR activity, as assessed by channel inhibition with Inh-172 following forskolin-induced activation. The change in CFTR-mediated Cl^- current, calculated as the difference between the absolute current value after inhibition and the forskolin-induced Cl^- current increase, was significantly lower in PS-NP-exposed monolayers compared with untreated controls (Fig. 5B). This observation may indicate a reduction in basal CFTR activity caused by PS-NPs. A small, but not significant,

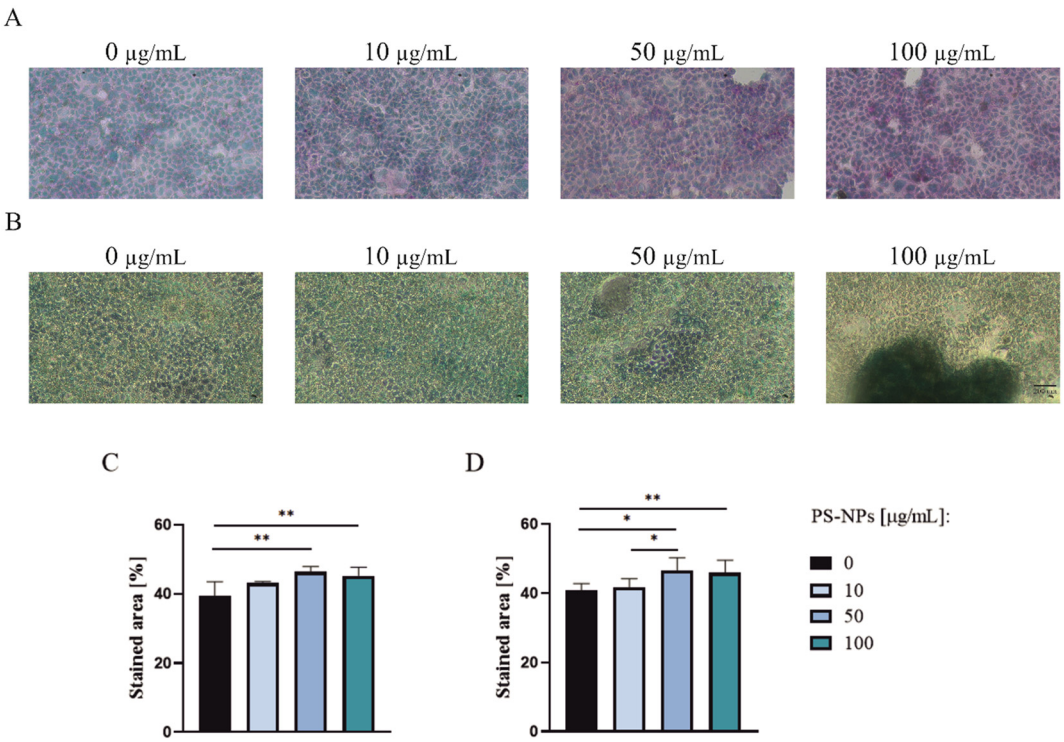

Fig. 4 Mucus staining in Caco-2 cells exposed to PS-NPs. (A) Alcian Blue/PAS staining of mucus in Caco-2 cells cultured on 96-well plates. (B) Alcian Blue staining of mucus in Caco-2 cells cultured on Transwell inserts. (C) Semi-quantitative analysis of the stained area [%] in cells grown on 96-well plates (n = 5). (D) Semi-quantitative analysis of the stained area [%] in cells grown on Transwell inserts (n = 5). Cells were exposed to PS-NPs at concentrations of 0, 10, 50, and 100 µg mL^{-1} for 72 h. Images were acquired using a DLTX1080PCMOSHDU2SD camera (DELTA Optical, Mińsk Mazowiecki, Poland) mounted on an inverted optical microscope (Olympus IMT-2, Tokyo, Japan). Stained area [%] was quantified using ImageJ software. Data are expressed as mean ± standard deviation (SD). Statistical significance was determined using Student's t-test. Significance levels: *$p < 0.05$, **$p < 0.05$.

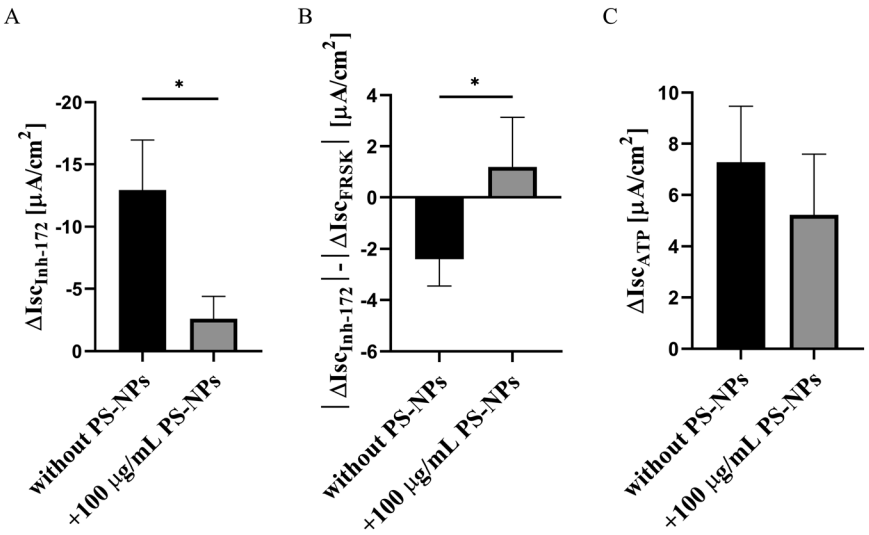

Fig. 5 Effect of 100 µg mL^{-1} PS-NPs on short-circuit Cl^- current in Caco-2 cell monolayers. (A) Effects of PS-NPs on CFTR activity assessed by the CFTR inhibition by Inh-172, following forskolin-induced activation. (B) Changes in CFTR channel activity, calculated as the difference between CFTR-mediated current inhibition after forskolin activation in PS-NP-treated and untreated Caco-2 monolayers. (C) Effect of PS-NPs presence on ATP-stimulated Cl^- currents. Data are expressed as mean ± SD (n = 3). Statistical significance relative to the control was determined using Student's t-test. Significance levels: *$p < 0.05$.

decrease in ATP-induced Cl^- current was also observed (Fig. 5C).

Acute apical addition of PS-NPs to the Ussing chamber induced a transient, concentration-dependent increase in Cl^- current (Fig. 6A). This suggested the activation of alternative apical ion channels. Based on the current characteristics, we hypothesized that calcium-activated chloride channel (CaCC) was implicated. To test this hypothesis, Ani-9 was added to the apical side of the cell monolayer prior to PS-NPs exposure. As shown in Fig. 6B, this treatment completely abolished the effect of PS-NPs observed in non inhibited cell monolayers, confirming the involvement of TMEM16A in response to PS-NPs. Treatment with Ani-9 alone did not alter the Isc, indicating that TMEM16A is not active under basal conditions (Fig. 6C).

3.6. Intracellular calcium level detection

Since the TMEM16A channel belongs to the family of calcium-dependend chloride channels family, the effect of PS-NPs on intracellular calcium homeostasis in Caco-2 cells was investigated by measuring changes in [Ca^{2+}] using the Fura-2 ratiometric dye. As shown in Fig. 7, the alterations in [Ca^{2+}] were observed, however, none of the concentrations used

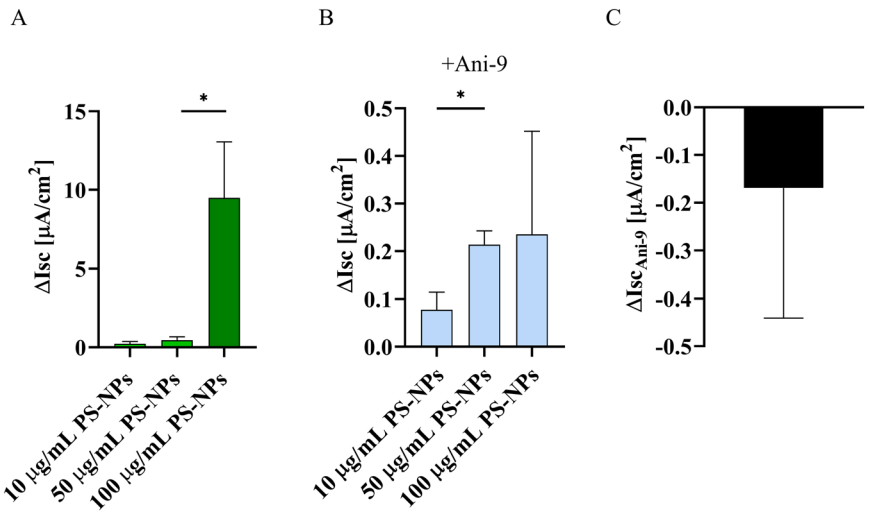

Fig. 6 Effect of acute PS-NPs exposure on short-circuit Cl^- current in Caco-2 cell monolayers. (A) Cl^- current change in the absence of Ani-9. (B) Cl^- current change in the presence of Ani-9. (C) The effect of Ani-9 on Cl^- current change. Data are expressed as mean ± SD (n = 3). Statistical significance was determined using Student's t-test. Significance levels: *$p < 0.05$.

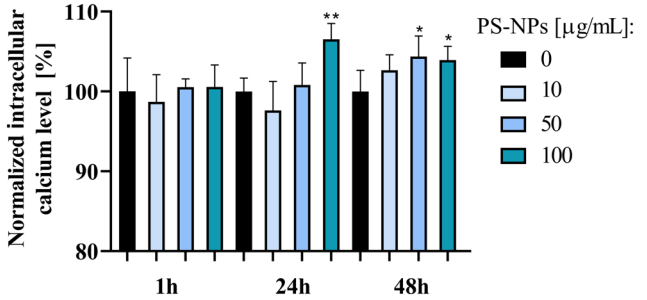

Fig. 7 Intracellular calcium levels in Caco-2 cells following PS-NP exposure. Cells were treated with 10, 50, 100 μg mL^{-1} PS-NPs for 1, 24, and 48 hours. Results were calculated as the fluorescent ratio of F340/F380 and presented as the mean ± SD (n = 6). Statistical significance was determined using one-way ANOVA. Significance levels: *$p < 0.05$, **$p < 0.01$.

changed the [Ca^{2+}] levels after 1 hour. Statistically significant changes were observed in cells treated with 50, 100 μg mL^{-1} of PS-NPs after 48 hours of incubation.

4. Discussion

Plastics are increasingly recognized as major environmental pollutants, with their presence documented across diverse ecosystems and raising concerns about potential risks to living organisms.[26] However, the precise mechanisms underlying these interactions remain poorly understood.[6] There is still limited experimental data concerning the effect of nanoplastic on intestinal epithelium, especially from the electrophysiological point of view. The data presented here suggests that polystyrene nanoplastic causes elevated TMEM16A channel activity, which can lead to enhanced mucus production by intestinal cells. The involvement of TMEM16A activity was demonstrated utilizing its specific inhibitor. Additionally, nanoplastic caused a decrease in CFTR channel activity, a transporting protein playing a paramount role in mucus expansion.

PS-NPs do not affect Caco-2 cells viability and proliferation

The cell viability results indicate that 100 nm PS-NPs do not exert cytotoxic effects on Caco-2 cells. Our findings are consistent with several studies reporting no or only mild cytotoxicity in Caco-2 cells exposed to PS-NPs of different sizes (50–100 nm, 200 nm) or larger microparticles (1, 2, 4, 5, and 10 μm) across a wide range of concentrations and exposure times (1–72 h).[27–29] However, some reports present conflicting results. Wu *et al.* observed no effect on Caco-2 viability after 24 h of exposure to 5 μm PS-NPs, but a mild reduction after 48 h.[30] Similarly, Xu *et al.* reported no toxicity in Caco-2 cells treated with 100 nm PS nanoparticles for 24 h, yet viability declined at the highest dose (480 μg mL^{-1}) after 48 h and at all tested doses following 96 h.[31] Interestingly, 100 nm PS-NPs disrupted plasma membrane integrity after 96 h, whereas 5 μm particles did not.[32] These findings suggest that the cytotoxic effects of PS-NPs are complex and dependent on both particle size and concentration. In contrast, another study on undifferentiated Caco-2 cells reported no toxicity, even after prolonged exposure for 7 days.[33]

In addition, no effect of PS-NPs on Caco-2 cell migration was detected in the scratch assay. Previous studies in lung cancer cell lines have demonstrated that PS-NPs can alter cell proliferation, either through inhibition or enhancement.[34,35] In contrast, our study showed no significant changes in the migration capacity of Caco-2 cells exposed to 100 nm PS-NPs at the tested concentrations. These findings suggest that cellular responses to nanoplastics are highly variable and depend on cell type or even specific cell lines, thereby adding to the complexity of their potential effects at the organismal level.

PS-NPs do not significantly affect the barrier integrity

A small but not significant increase in TEER after 24, 48, and 72 h, indicated that the integrity of Caco-2 monolayers remained preserved following PS-NPs treatment. These findings are consistent with previous reports.[33,36,37] For example, Marcellus *et al.* observed no significant effect on either Caco-2 monocultures or Caco-2/HT29-MTX/THP-1 tri-cultures exposed to different PS-NPs sizes (50 nm, 500 nm, 1 μm) for 24 h.[33] Additionally, Choi *et al.* reported an increase in TEER in Caco-2 monolayers treated with polystyrene particles (50, 100, 500 nm) after 24 and 48 h, followed by a decrease after 72 h.[37] The cause of this decline remains unclear, as viability assays indicated no cytotoxicity of polystyrene. Moreover, the barrier integrity of the Caco-2 monoculture was functionally preserved, as shown by intact ZO-1 organization, suggesting that tight junctions remained structurally resilient despite particle exposure.[37] Similar findings were reported in intestinal organoid-derived epithelial tissue models, where TEER values declined only upon exposure to smaller PS-NPs (30 nm) or to high concentrations (1000 μg mL^{-1}) of 100 nm PS-NPs.[38]

Transient TEER fluctuations may reflect subtle alterations in ion transport, membrane permeability, or paracellular conductance rather than overt disruption of tight junction complexes. This suggests that PS-NPs can induce mild, reversible functional changes without compromising the structural integrity of epithelial barriers, although prolonged or high-dose exposure may eventually destabilize junctional regulation.

PS-NPs increase mucus production in Caco-2 cells

In recent years, the intestinal mucus layer has received increasing attention as a key component of the intestinal barrier and a regulator of gut homeostasis. Secreted by epithelial cells, it protects from chemical insults, environmental pollutants, and pathogenic microorganisms, while also provides hydration that safeguards against mechanical damage.[39,40] Dysregulated mucus production disrupts intestinal and systemic homeostasis: excess mucus

can trigger inflammation, alter microbiota, and increase infection risk,[41,42] while insufficient mucus weakens the barrier by increasing epithelial permeability and making the gut more vulnerable to inflammation and infection. In addition, inadequate mucus impairs nutrient absorption and may contribute to gastrointestinal disorders.[43,44]

Our results show that exposure of Caco-2 cells to PS-NPs induced a concentration-dependent increase in mucus production. Formation of mucus plugs suggests that PS-NPs trigger mucus hypersecretion. Such hypersecretion may represent a defensive mechanism aimed at limiting particle penetration; however, it could also result in mucus accumulation, altered barrier properties, and disrupted host–microbiota interactions.[45] Importantly, these effects may pose a greater health risk in individuals with a compromised intestinal mucus barrier.[46] Similar findings have been reported in other studies, where nanoplastic exposure was shown to stimulate mucin expression as part of a protective epithelial response. For instance, Cui *et al.* demonstrated, in both *in vitro* and *in vivo* models, that exposure to 20 nm nanoplastics significantly increased MUC2 protein expression in the intestinal epithelium.[47] Interestingly, in contrast to our findings, several rodent studies have reported reduced mucus secretion following oral nanoplastic exposure, indicating that the impact of PS-NPs on mucus regulation may depend on model system, exposure route, or species-specific differences.[48,49]

PS-NPs alter ion transport across Caco-2 cell monolayers

Our short-circuit current data suggests that PS-NPs can modulate the activity of epithelial ion channels, particulary CFTR and TMEM16A, which mediate Cl^- secretion and drive water movement into the intestinal lumen.[50–52] The inhibitory effect on CFTR channel is particularly interesting, as CFTR mediates bicarbonate secretion, which is critical for mucus expansion and proper barrier function.[53–55] Disruption of CFTR-mediated ion transport can therefore alter mucus viscosity, compromise epithelial protection, and disturb host–microbiota interactions.[56] The dense, cell-attached mucus plugs observed in PS-NPs treated Caco-2 monolayers may thus result from reduced bicarbonate secretion, which impairs mucus expansion, and when combined with hypersecretion, leads to abnormal mucus accumulation.

TMEM16A has been also shown to play an indispensable role in mucus secretion[15] as well as gastrointestinal motility.[57] Our data show that PS-NPs activate the TMEM16A channel, which might be associated with increased mucus secretion. Furthermore, intracellular Ca^{2+} levels—known activators of TMEM16A[57] —were significantly elevated in cells exposed to PS-NPs.

In this study, we focused primarily on the acute effects of PS-NPs on ion transport. In contrast, previous studies have shown that prolonged exposure of intestinal cells to PS-NPs can alter both the expression and protein levels of multiple ion transporters.[58] Consistent with these findings, PS-NPs-treated mice exhibited significantly reduced mRNA levels of *Ano1*, *Cftr*, *Slc26a3*, *Slc26a6*, *Nkcc1*, and *Nhe3* compared with untreated controls.[58] Collectively, these results highlight the need for future studies to investigate the long-term effects of PS-NPs on the regulation of a broader spectrum of ion transport proteins.

Clinical consequences of findings

Together, our findings suggest that PS-NP exposure may subtly alter intestinal epithelial function in humans. Reduced CFTR activity may lead to thicker, denser mucus, similar to that observed in CFTR-dysfunction states. A chronic mucus-hypersecretory phenotype without overt epithelial injury could progressively impair intestinal barrier function. An altered CFTR/TMEM16A balance may reduce mucus clearance, increasing susceptibility to low-grade inflammation, dysbiosis, or enhanced uptake of luminal irritants without causing acute toxicity. It is therefore likely that PS-NP exposure may exacerbate pre-existing gastrointestinal conditions rather than induce disease *de novo*.

5. Study limitations

In this study, we provide new insights into the effects of PS-NPs on Caco-2 cells; however, it is not without limitations. First, the experiments were conducted in a simplified *in vitro* monoculture model, which cannot fully replicate the complexity of the intestinal environment, including interactions with immune cells, microbiota, and mucus dynamics *in vivo*. Second, only one nanoparticle type (100 nm PS) was tested, whereas environmental exposure involves a wide range of plastic sizes, shapes, surface chemistries, and additives that may differentially affect epithelial responses. Third, the concentrations and exposure times used in this study may not directly reflect real-world exposure scenarios, which limits extrapolation to human health risk. Finally, the study primarily focused on acute effects, leaving the long-term consequences of chronic, low-dose exposure unresolved. Future research should therefore employ co-culture systems, intestinal organoids, and *in vivo* models to better capture the physiological relevance of nanoplastic exposure.

6. Conclusions

Limited electrophysiological data are available on how nanoplastics interact with the human intestinal epithelium, creating uncertainty about their potential health impact. Our study demonstrates that, although polystyrene nanoplastics do not induce direct cytotoxicity or compromise epithelial monolayer integrity, they do modulate the activity of two chloride-secreting channels, leading to increased mucus secretion. These findings provide novel mechanistic insights into interactions between PS-NPs and epithelium, contribute to a better understanding of their potential biological consequences.

Author contributions

Conceptualization, M. Z. and P. B.; methodology, G. W. and M. Z.; validation, M. Z., P. B., and G. W.; formal analysis, M. Z. and G. W.; investigation, G. W., M. Z.; resources, P. B., M. Z.; data curation, G. W., M. Z., J. H.; writing – original draft preparation, G. W. and M. Z.; writing – review and editing, M. Z., G. W., J. H. and P. B.; visualization, G. W. and M. Z.; supervision, M. Z. and P. B.; project administration, M. Z.; funding acquisition, P. B and M. Z. All authors have read and agreed to the published version of the manuscript.

Conflicts of interest

There are no conflicts of interest to declare.

Data availability

All data generated or analyzed during the current study are included. Illustration has been created in BioRender.

Acknowledgements

This work was financed by an OPUS 27 grant (No. 2024/53/B/NZ3/01635) (PB) from the National Science Centre (NCN), Poland, System of Financial Support for Scientists and Research Teams – SGGW (Warsaw University of Life Sciences) No. SWF/2/2024 (MZ). The publication was (co)financed by Science development fund of the Warsaw University of Life Sciences – SGGW.

References

1 Plastics-the Facts 2021, Plastics Europe 2021. Available from https://plasticseurope.org/knowledge-hub/plastics-the-facts-2021/, (Accessed January 2025).
2 L. Nizzetto and S. Sinha, *One Earth*, 2020, **2**, 11–15.
3 P. G. C. Nayanathara Thathsarani Pilapitiya and A. S. Ratnayake, *Cleaner Mater.*, 2024, **11**, 100220.
4 I. Donisi, A. Colloca, C. Anastasio, M. L. Balestrieri and N. D'onofrio, *Int. J. Biol. Sci.*, 2024, **20**, 5779–5792.
5 H. Li, L. Bai, S. Liang, X. Chen, X. Gu, C. Wang and C. Gu, *Eco-Environ. & Health*, 2025, **4**, 100138.
6 A. Nawab, M. Ahmad, M. T. Khan, M. Nafees, I. Khan and I. Ihsanullah, *J. Hazard. Mater. Adv.*, 2024, **16**, 100487.
7 J. C. Prata, J. P. da Costa, I. Lopes, A. C. Duarte and T. Rocha-Santos, *Sci. Total Environ.*, 2020, **702**, 134455.
8 Y. C. Chen, K. F. Chen, K. Y. Andrew Lin, H. P. Su, D. N. Wu and C. H. Lin, *Chemosphere*, 2023, **313**, 137582.
9 T. Stalder, T. Zaiter, W. El-Basset, R. Cornu, H. Martin, M. Diab-Assaf and A. Béduneau, *Toxicology*, 2022, **481**, 153353.
10 C. Song, Z. Chai, S. Chen, H. Zhang, X. Zhang and Y. Zhou, *Exp. Mol. Med.*, 2023, **55**, 681–691.
11 J. Gao, B. Cao, R. Zhao, H. Li, Q. Xu and B. Wei, *Pharmaceuticals*, 2023, **16**, 1216.
12 G. C. Hansson, *J. Intern. Med.*, 2019, **285**, 479–490.
13 Y. Hu and B. Tuo, *Int. J. Mol. Med.*, 2025, **55**, 99.
14 N. Yang, M. A. S. Garcia and P. M. Quinton, *J. Physiol.*, 2013, **591**, 4581–4593.
15 R. Benedetto, I. Cabrita, R. Schreiber and K. Kunzelmann, *FASEB J.*, 2019, **33**, 4502–4512.
16 A. Amobonye, P. Bhagwat, S. Raveendran, S. Singh and S. Pillai, *Front. Microbiol.*, 2021, **12**, 768297.
17 T. Gouin, R. Ellis-Hutchings, M. Pemberton and B. Wilhelmus, *Part. Fibre Toxicol.*, 2024, **21**, 1–27.
18 A. Kustra, M. Zając, P. Bednarczyk and K. Maliszewska-Olejniczak, *Biol. Res.*, 2025, **58**, 1–16.
19 Y. Sambruy, S. Ferruzza, G. Ranaldi and I. De Angelis, *Cell Biol. Toxicol.*, 2001, **17**, 301–317.
20 T. Lea, *The Impact of Food Bioactives on Health: In Vitro and Ex Vivo Models*, 2015, pp. 103–111.
21 S. M. Hammoudeh, A. M. Hammoudeh and R. Hamoudi, *Histochem. Cell Biol.*, 2019, **152**, 75–84.
22 J. Hoser, G. Weglinska, A. Samsel, K. Maliszewska-Olejniczak, P. Bednarczyk and M. Zajac, *Int. J. Mol. Sci.*, 2024, **25**, 11999.
23 S. Aliya, M. Alhammadi, S. Ilangovan, S. Han, S. Tamang, B. Son, H. U. Lee and Y. S. Huh, *Environ. Chem. Ecotoxicol.*, 2025, **7**, 706–728.
24 F. Jahedi and N. Jaafarzadeh Haghighi Fard, *Toxicol. Rep.*, 2025, **14**, 102043.
25 K. Senathirajah, S. Attwood, G. Bhagwat, M. Carbery, S. Wilson and T. Palanisami, *J. Hazard. Mater.*, 2021, **404**, 124004.
26 M. Hossain and I. Engelhardt, *Energy, Ecol. Environ.*, 2025, **10**, 637–674.
27 M. Peng, M. Vercauteren, C. Grootaert, A. Rajkovic, N. Boon, C. Janssen and J. Asselman, *Environ. Pollut.*, 2023, **337**, 122550.
28 C. Cortés, J. Domenech, M. Salazar, S. Pastor, R. Marcos and A. Hernández, *Environ. Sci.:Nano*, 2020, **7**, 272–285.
29 B. Wu, X. Wu, S. Liu, Z. Wang and L. Chen, *Chemosphere*, 2019, **221**, 333–341.
30 S. Wu, M. Wu, D. Tian, L. Qiu and T. Li, *Environ. Toxicol.*, 2020, **35**, 495–506.
31 D. Xu, Y. Ma, X. Han and Y. Chen, *J. Hazard. Mater.*, 2021, **417**, 126092.
32 S. Liu, X. Wu, W. Gu, J. Yu and B. Wu, *Chemosphere*, 2020, **256**, 127204.
33 K. A. Marcellus, D. Prescott, M. Scur, N. Ross and S. S. Gill, *Nanomaterials*, 2025, **15**, 267.
34 B. Ernhofer, A. Spittler, F. Ferk, M. Mišík, M. M. Zylka, L. Glatt, K. Boettiger, A. Solta, D. Kirchhofer, G. Timelthaler, Z. Megyesfalvi, V. Kopatz, H. Kovar, S. Knasmueller, C. Aigner, L. Kenner, B. Döme and K. Schelch, *J. Hazard. Mater.*, 2025, **495**, 139129.
35 B. Annangi, A. Villacorta, M. López-Mesas, V. Fuentes-Cebrian, R. Marcos and A. Hernández, *Biomolecules*, 2023, **13**, 220.
36 M. B. Paul, L. Böhmert, I. L. Hsiao, A. Braeuning and H. Sieg, *Environ. Int.*, 2023, **179**, 108172.
37 H. Choi, S. Kaneko, Y. Suzuki, K. Inamura, M. Nishikawa and Y. Sakai, *Nanomaterials*, 2024, **14**, 1435.

38 Y. Chen, A. M. Williams, E. B. Gordon, S. E. Rudolph, B. N. Longo, G. Li and D. L. Kaplan, *Nanomedicine*, 2023, **50**, 102680.
39 M. Shimizu, *Biosci., Biotechnol., Biochem.*, 2010, **74**, 232–241.
40 C. Q. Y. Yong, S. Valiyaveettil and B. L. Tang, *Int. J. Environ. Res. Public Health*, 2020, **17**, 1509.
41 M. Naama, S. Telpaz, A. Awad, A. Nyska, M. Nuriel-Ohayon, S. B. Correspondence, S. Ben-Simon, S. Harshuk-Shabso, S. Modilevsky, E. Rubin, J. Sawaed, L. Zelik, M. Zigdon, N. Asulin, S. Turjeman, M. Werbner, S. Wongkuna, R. Feeney, B. O. Schroeder and S. Bel, *Cell Host Microbe*, 2023, **31**, 433–446.
42 R. Okumura and K. Takeda, *Inflammation Regener.*, 2018, **38**, 5.
43 J. Damianos, N. Abdelnaem and M. Camilleri, *Clin. Gastroenterol. Hepatol.*, 2024, **23**, 205–215.
44 S. Li, M. Chen, Z. Wang, W. Abudourexiti, L. Zhang, C. Ding, L. Ding and J. Gong, *Microbiol. Res.*, 2024, **281**, 127599.
45 W. H. Hsu, Y. Z. Chen, Y. T. Chiang, Y. T. Chang, Y. W. Wang, K. T. Hsu, Y. Y. Hsu, P. T. Wu and B. H. Lee, *Nat. Commun.*, 2025, **16**, 1–13.
46 A. Bruno, M. Dovizio, C. Milillo, E. Aruffo, M. Pesce, M. Gatta, P. Chiacchiaretta, P. Di Carlo and P. Ballerini, *Cancers*, 2024, **16**, 3079.
47 M. Cui, Q. He, Z. Wang, Y. Yu, H. Gao, Z. Liu, H. Peng, H. Wang, X. Zhang, D. Li, L. Chen, X. Xing, Y. Xiao, W. Chen and Q. Wang, *Environ. Pollut.*, 2023, **330**, 121808.
48 H. Sun, N. Chen, X. Yang, Y. Xia and D. Wu, *Ecotoxicol. Environ. Saf.*, 2021, **220**, 112340.
49 X. Chen, J. Zhuang, Q. Chen, L. Xu, X. Yue and D. Qiao, *Ecotoxicol. Environ. Saf.*, 2022, **241**, 113809.
50 C. Li and A. P. Naren, *Integr. Biol.*, 2010, **2**, 161–177.
51 M. Zajac and K. Dolowy, *Prog. Biophys. Mol. Biol.*, 2017, **127**, 1–11.
52 Y. D. Yang, H. Cho, J. Y. Koo, M. H. Tak, Y. Cho, W. S. Shim, S. P. Park, J. Lee, B. Lee, B. M. Kim, R. Raouf, Y. K. Shin and U. Oh, *Nature*, 2008, **455**, 1210–1215.
53 E. Y. T. Chen, N. Yang, P. M. Quinton and W. C. Chin, *Am. J. Physiol.*, 2010, **299**, 542–549.
54 M. Zajac, E. Dreano, A. Edwards, G. Planelles and I. Sermet-Gaudelus, *Int. J. Mol. Sci.*, 2021, **22**, 3384.
55 M. Zajac, A. Lepissier, E. Dréano, B. Chevalier, A. Hatton, M. Kelly-Aubert, D. Guidone, G. Planelles, A. Edelman, E. Girodon, A. Hinzpeter, G. Crambert, I. Pranke, L. J. V. Galietta and I. Sermet-Gaudelus, *Front. Pharmacol.*, 2023, **14**, 1293578.
56 A. K. Purushothaman and E. J. R. Nelson, *Heliyon*, 2023, **9**, e17553.
57 Q. Ji, S. Guo, X. Wang, C. Pang, Y. Zhan, Y. Chen and H. An, *J. Cell. Physiol.*, 2019, **234**, 7856–7873.
58 Y. Jin, L. Lu, W. Tu, T. Luo and Z. Fu, *Sci. Total Environ.*, 2019, **649**, 308–317.